JACS
JOURNAL OF THE AMERICAN CHEMICAL SOCIETY
Communication
pubs.acs.org/JACS

One-Electron Activation of Water Oxidation Catalysis

Yusuke Tamaki, Aaron K. Vannucci, Christopher J. Dares, Robert A. Binstead, and Thomas J. Meyer*

Department of Chemistry, University of North Carolina at Chapel Hill, CB 3290, Chapel Hill, North Carolina 27599, United States

Supporting Information

ABSTRACT: Rapid water oxidation catalysis is observed following electrochemical oxidation of $[Ru^{II}(tpy)(bpz)(OH)]^{+}$ to $[Ru^{V}(tpy)(bpz)(O)]^{3+}$ in basic solutions with added buffers. Under these conditions, water oxidation is dominated by base-assisted Atom Proton Transfer (APT) and direct reaction with OH^{-}. More importantly, we report here that the $Ru^{IV}{=}O^{2+}$ form of the catalyst, produced by $1e^{-}$ oxidation of $[Ru^{II}(tpy)(bpz)(OH_2)]^{2+}$ to Ru(III) followed by disproportionation to $[Ru^{IV}(tpy)(bpz)(O)]^{2+}$ and $[Ru^{II}(tpy)(bpz)(OH_2)]^{2+}$, is also a competent water oxidation catalyst. The rate of water oxidation by $[Ru^{IV}(tpy)(bpz)(O)]^{2+}$ is greatly accelerated with added PO_4^{3-} with a turnover frequency of 5.4 s^{-1} reached at pH 11.6 with 1 M PO_4^{3-} at an overpotential of only 180 mV.

In water oxidation there is a requirement for $4e^{-}/4H^{+}$ loss and O···O bond formation, eq 1. The multielectron/multiproton nature of the reaction ensures that water oxidation mechanisms are complex with mechanistic details and the rate-limiting step or steps dependent on the catalyst and reaction conditions.[1−19]

$$2H_2O - 4e^{-} - 4H^{+} \rightarrow O_2 \quad (1)$$

Detailed mechanistic insight is available. The single-site mechanism in Scheme 1 has been established for the Ru(II) polypyridyl complexes $[Ru(tpy)(bpm)(OH_2)]^{2+}$ (tpy = 2,2′:6′,2″-terpyridine, bpm = 2,2′-bipyrimidine) and $[Ru(tpy)(bpz)(OH_2)]^{2+}$ (bpz = 2,2′−bipyrazine) based on the results of kinetic and theoretical studies.[5,6]

As commonly found for these catalysts, the rate-limiting step in catalytic water oxidation cycles is O···O bond formation. PCET oxidation of $Ru^{II}{-}OH_2^{2+}$ to $Ru^{IV}{=}O^{2+}$ is followed by further oxidation to d^3 $Ru^{V}(O)^{3+}$. $E^{\circ\prime}$ values for the $Ru^{V}(O)/Ru^{IV}{=}O$ couples are typically >1.6 V, and reaching the reactive form of the catalyst is thermodynamically and mechanistically demanding requiring the loss of $3e^{-}$ and $2H^{+}$.

For the bpz complex $[Ru(tpy)(bpz)(OH_2)]^{2+}$ in Scheme 1, the potential for the $2e^{-}$ $Ru^{IV}{=}O^{2+}/Ru^{II}{-}OH_2^{2+}$ couple is 0.87 V at pH 7.[5,6,20] Water oxidation, $2Ru^{IV}{=}O^{2+} + 2H_2O \rightarrow 2Ru^{II}{-}OH_2^{2+} + O_2$, is thermodynamically favored, but by only 0.05 V. Initial oxidation of $Ru^{II}{-}OH_2^{2+}$ occurs by $2e^{-}$ to give $Ru^{IV}{=}O^{2+}$ with Ru(III) a "missing oxidation state", unstable toward disproportionation from pH 0−14. The thermodynamic instability of Ru(III) is due to stabilization of Ru(II) by $d\pi(Ru^{II})-\pi^{*}(bpz)$ backbonding which increases $E^{\circ\prime}$ for the Ru(III/II) couple above $E^{\circ\prime}$ for the Ru(IV/III) potential.[20,21] This means that electron transfer oxidation of $Ru^{II}{-}OH_2^{2+}$ to $Ru^{IV}{=}O^{2+}$ occurs by initial $1e^{-}$ oxidation to Ru(III), as $Ru^{III}{-}OH_2^{3+}$ or $Ru^{III}{-}OH^{2+}$ depending on pH, followed by further oxidation to $Ru^{IV}{=}O^{2+}$. Ru(III) does not build up as an intermediate since $E^{\circ\prime}(Ru(III)/[Ru^{II}{-}OH_2]^{2+}) > E^{\circ\prime}([Ru^{IV}{=}O]^{2+}/Ru(III))$. We have demonstrated disproportionation experimentally by initial mixing experiments in 0.05 M $HClO_4$. Stoichiometric oxidation of $[Ru^{II}(tpy)(bpz)(OH_2)]^{2+}$ to Ru(III) by $[Ru^{III}(bpy)_3]^{3+}$ is followed by disproportionation, 2 Ru(III) → $[Ru^{II}(tpy)(bpz)(OH_2)]^{2+}$ + $[Ru^{IV}(tpy)(bpz)(O)]^{2+}$, which occurs with $k \sim 47$ M^{-1} s^{-1}.

When combined, thermodynamic competence toward water oxidation by $Ru^{IV}{=}O^{2+}$ and thermodynamic instability of Ru(III) toward disproportionation raise the interesting possibility of reaching the rate-limiting, O···O bond forming step in Scheme 1 by *single electron activation* with $Ru^{IV}{=}O^{2+}$ as the oxidant rather than $Ru^{V}(O)^{3+}$. In a mechanism of this kind, initial oxidation to Ru(III),

$$Ru^{II}{-}OH_2^{2+} \xrightarrow{-e^{-}} Ru(III)$$

would be followed by disproportionation, 2Ru(III) → $Ru^{II}{-}OH_2^{2+}$ + $Ru^{IV}{=}O^{2+}$, to give the active form of the catalyst. A $Ru^{IV}{=}O^{2+}$ mechanism would have the added advantage of a

Scheme 1. Single-Site Water Oxidation Mechanism for $[Ru(tpy)(bpz)(OH_2)]^{2+}$ [5,6]

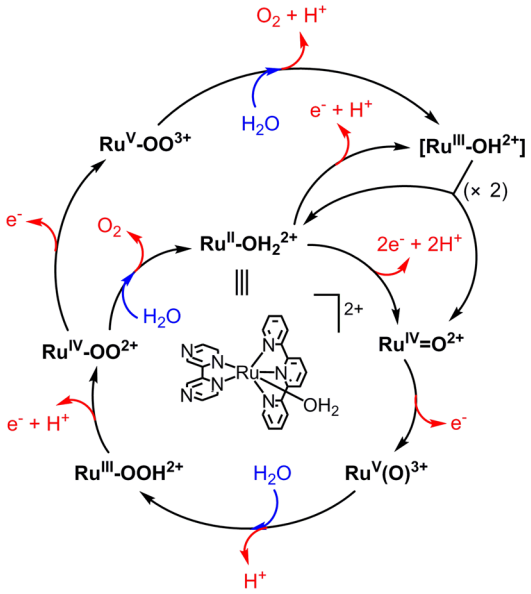

Received: March 14, 2014
Published: April 23, 2014

   dx.doi.org/10.1021/ja502637s | J. Am. Chem. Soc. 2014, 136, 6854−6857

considerable decrease in overpotential for water oxidation.[14] Single electron activation could be especially important in photochemical and photoelectrochemical water oxidation with water oxidation driven by single photon/single electron transfer with the sequential buildup of multiple oxidative equivalents for water oxidation.

We report here that water oxidation catalysis does occur for $[Ru^{IV}(tpy)(bpz)(O)]^{2+}$ but at significant rates only with added bases, which enhance O···O coupling by a combination of Atom-Proton Transfer (APT) and direct reaction with OH^-.[7−9] Under these conditions, sustained water oxidation catalysis occurs at reasonable rates with low overpotentials.

$[Ru(tpy)(bpz)(OH_2)](PF_6)_2$ (**Ru^{II}−OH_2^{2+}**) was synthesized by a literature procedure.[5] Mixing experiments for $[Ru(tpy)(bpz)(OH_2)]^{2+}$ with added Ce^{IV} as oxidant in 0.5 M $HClO_4$ at room temperature with spectrophotometric monitoring reveal that water oxidation by $[Ru^{IV}(tpy)(bpz)(O)]^{2+}$ is slow in acidic solutions, occurring on a time scale of minutes by a complex mechanism or mechanisms. In earlier work, we demonstrated catalysis of water oxidation by $Ru^V(O)$ assisted by added bases, CH_3COO^-, $H_2PO_4^-$, and HPO_4^{2-}, by utilization of APT.[7,8] As illustrated in eq 2, APT is a concerted process in which a proton acceptor base (B) removes a proton in concert with O···O bond formation, in this case, to form a Ru(III) hydroperoxide intermediate.[7−9]

$$Ru^V(O)^{3+} + HOH\cdots B \rightarrow Ru^{III}{-}OOH^{2+} + HB^+ \quad (2)$$

For electrochemistry, catalyzed water oxidation was investigated by electrochemical measurements in phosphate buffers with added KNO_3 at an ionic strength of 0.25 at room temperature. For kinetic measurements, a 0.07 cm^2 boron-doped diamond (BDD) electrode was used as the working electrode. For controlled potential electrolysis experiments with oxygen detection, a reticulated vitreous carbon electrode was used that had been surface modified by addition of nanoparticle indium tin oxide (*nano*ITO−RVC) (Figure S1).[22]

Figure 1 shows a series of current-normalized cyclic voltammograms ($i/\nu^{1/2}$ with ν = scan rate) for **Ru^{II}−OH_2^{2+}** at pH 6.7 ($H_2PO_4^-/HPO_4^{2-}$ + KNO_3, I = 0.25) and for **Ru^{II}−OH^+** at pH 11.6 (HPO_4^{2-}/PO_4^{3-} + KNO_3, I = 0.25) at scan rates from ν = 10 to 400 mV/s at room temperature. For the coordinated water in $[Ru^{II}(tpy)(bpz)(OH_2)]^{2+}$, pK_a = 8.8.[20] At pH 6.7, normalized currents for the $Ru^{IV}{=}O^{2+}/Ru^{II}{-}OH_2^{2+}$ wave were nearly independent of scan rate consistent with the Randles-Sevcik relationship in eq 3. Under these conditions, there was no evidence for water oxidation catalysis by $Ru^{IV}{=}O^{2+}$ on the CV time scale. In eq 3, i_p is the peak current, [**Ru^{II}−OH_2^{2+}**] is the concentration of complex, n is the number of electrons transferred with n = 2 for oxidation of $Ru^{II}{-}OH_2^{2+}$ to $Ru^{IV}{=}O^{2+}$. D is the diffusion coefficient for **Ru^{II}−OH_2^{2+}** with $D = 1.1 \times 10^{-7}$ cm^2/s ($H_2PO_4^-/HPO_4^{2-}$ + KNO_3, I = 0.25) as obtained from the plot of $i_{p,a}$ vs $\nu^{1/2}$ in Figure S2 and eq 3. The peak-to-peak potential separation, $\Delta E_p = E_{p,a} - E_{p,c}$, with $E_{p,a}$ and $E_{p,c}$ the anodic and cathodic peak potentials, increases with increasing scan rate from 140 mV at 10 mV/s to 420 mV at 400 mV/s consistent with kinetically inhibited, diffusional electron transfer for the 2e⁻ couple at the electrode.

$$i_p = 0.446nFA[\mathbf{Ru^{II}{-}OH_2^{2+}}](nF\nu D/RT)^{1/2} \quad (3)$$

Continuation of oxidative scans to $E_{p,a}$ = 1.6 V with oxidation to $Ru^V(O)^{3+}$ provides clear evidence for scan rate dependent current increases and catalytic water oxidation, see below.

By contrast, at pH 11.6 with $[PO_4^{3-}]$ = 5.9 mM, there is clear evidence in Figure 1b for a scan rate dependence in the normalized oxidative current for the

$$Ru^{II}{-}OH^+ \xrightarrow{-2e^-,-H^+} Ru^{IV}{=}O^{2+}$$

wave and for catalytic water oxidation by both $Ru^V(O)^{3+}$ and $Ru^{IV}{=}O^{2+}$. To confirm that catalyzed water oxidation was occurring, we carried out controlled potential electrolysis at 1.6 V, $E_{p,c}$ for oxidation of $Ru^{IV}{=}O^{2+}$ to $Ru^V(O)^{3+}$ in a HPO_4^{2-}/PO_4^{3-} buffer ($[PO_4^{3-}]$ = 5.9 mM) at pH 11.6, I = 0.25 (HPO_4^{2-}/PO_4^{3-} + KNO_3) with 1 mM **Ru^{II}−OH^+**. Following electrolysis periods of 15−30 s, reductive CV scans at the same working electrode revealed the presence of O_2 by the appearance of the characteristic O_2 reduction wave at $E_{p,c} \sim -0.5$ V. Qualitatively, the magnitude of the peak current increased with electrolysis time. Electrolysis at 0.9 V with water oxidation by $Ru^{IV}{=}O^{2+}$ failed to reveal a reductive wave for O_2 because of the decreased rate of O_2 formation and loss of O_2 from the interface by diffusion (Figure S3). Controlled potential electrolysis at a high surface area *nano*ITO−RVC electrode[22] under the same conditions at 0.9 V for 1 h occurred with 1.4 turnovers per catalyst to give O_2 with a faradaic efficiency of 84% by GC analysis of the head space in the electrolysis cell corrected for dissolved oxygen (Figure S4). The catalyst was stable under the conditions of the electrolysis as shown by UV−visible measurements before and after electrolysis (Figure S5).

The dependence of the catalytic currents for water oxidation by both $Ru^{IV}{=}O^{2+}$ and $Ru^V(O)^{3+}$ on $[PO_4^{3-}]$ and $[OH^-]$ was investigated by catalytic current measurements at 0.9 and 1.6 V at room temperature in phosphate buffers at I = 0.25 (HPO_4^{2-}/PO_4^{3-} + KNO_3) at the 0.07 cm^2 BDD electrode. After 100 s, stable catalytic plateau currents were reached (Figure S6a) and analyzed by eq 4. In eq 4, i_{cat} is the sustained catalytic current, k_{obs} is the observed rate constant for water oxidation catalysis, D = 1.1×10^{-7} cm^2/s from the scan rate dependent CV measurements, and n = 4 for water oxidation. From this value for D and the slope of the plot in Figure S6b, k_{obs} = 0.17 s^{-1} at 0.9 V at pH 11.6 with $[PO_4^{3-}]$ = 5.9 mM.

$$i_{cat} = nFA[\mathbf{Ru^{II}{-}OH^+}](Dk_{obs})^{1/2} \quad (4)$$

The dependence of k_{obs} on phosphate concentration from 1.8−12 mM at pH 11.6 was investigated by varying the total

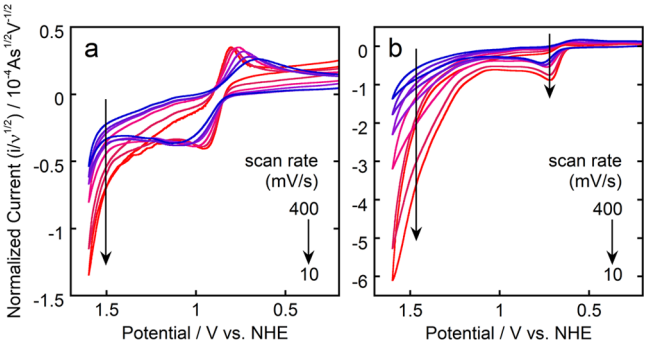

Figure 1. Normalized ($i/\nu^{1/2}$) cyclic voltammograms for **Ru^{II}−OH_2^{2+}** (1 mM) in a phosphate buffer at pH 6.7 (a, $H_2PO_4^-/HPO_4^{2-}$ + KNO_3, I = 0.25) and for **Ru^{II}−OH^+** (1 mM) at pH 11.6 (b, HPO_4^{2-}/PO_4^{3-} + KNO_3, I = 0.25) at scan rates from 10 to 400 mV/s at a BDD working electrode (0.07 cm^2) illustrating current increases with decreasing scan rate.

dx.doi.org/10.1021/ja502637s | J. Am. Chem. Soc. 2014, 136, 6854−6857

buffer concentration at constant buffer ratios, $[HPO_4^{2-}]/[PO_4^{3-}]$, with the results shown in Figure 2a. On the basis of these data, k_{obs} for water oxidation by $Ru^{IV}{=}O^{2+}$ increases linearly with $[PO_4^{3-}]$ consistent with the rate constant expression, $k_{obs,Ru(IV)} = k_0 + k_{Ru(IV),PO4}[PO_4^{3-}]$ with $k_{Ru(IV),PO4}$ = 5.4 M^{-1} s^{-1} as determined from the slope with k_0 = 0.15 s^{-1} from the intercept.

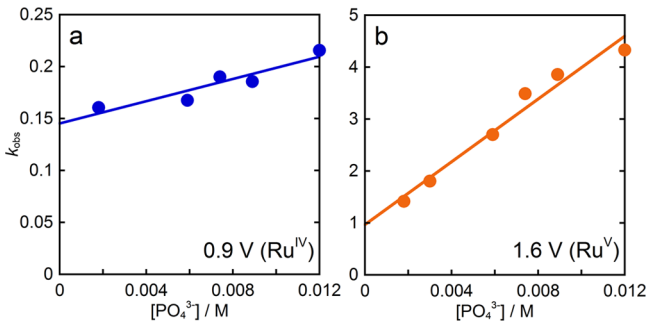

Figure 2. Plots of k_{obs} vs $[PO_4^{3-}]$ for $Ru^{IV}{=}O^{2+}$ (a) and $Ru^{V}(O)^{3+}$ (b) at pH 11.6, I = 0.25 at room temperature.

In parallel experiments with i_{cat} measurements at 1.6 V for water oxidation by $Ru^{V}(O)^{3+}$ (Figure S7), k_{obs} was also found to vary linearly with $[PO_4^{3-}]$, Figure 2b. From the slope of a plot of $k_{obs,Ru(V)}$ vs $[PO_4^{3-}]$, $k_{Ru(V),PO4} = 3.0 \times 10^2$ M^{-1} s^{-1} and k_0 = 0.97 s^{-1} (Figure 2b). Corrections for oxidation by $Ru^{IV}{=}O^{2+}$ were negligible under these conditions. In a recent paper on water oxidation by a related Ru(II) polypyridyl complex with added Britton-Robinson buffer, a pH-dependent water oxidation onset was observed past the $Ru^{IV}{=}O^{2+}/Ru^{II}{-}OH_2^{2+}$ wave and attributed to electron transfer from $Ru^{IV}{=}O^{2+}$ to the electrode in concert with O···O bond formation.[14] Given our results, with water oxidation by both $Ru^{V}(O)^{3+}$ and $Ru^{IV}{=}O^{2+}$, and the enhanced reactivity of $Ru^{V}(O)^{3+}$ compared to $Ru^{IV}{=}O^{2+}$, the origin of the apparent pH dependence with the added buffer mixture in the earlier work may be the same as found here. Its origin may lie in base catalyzed APT oxidation by $Ru^{V}(O)^{3+}$ with the concentration of acceptor base(s) in the buffer mixture increasing as the pH was increased.

For atom-proton transfer, the appearance of the term first order in $[PO_4^{3-}]$ for both $Ru^{V}(O)^{3+}$ and $Ru^{IV}{=}O^{2+}$ is consistent with APT water oxidation with PO_4^{3-} as the acceptor base, eq 5. The considerable rate enhancement for $Ru^{V}(O)^{3+}$ compared to $Ru^{IV}{=}O^{2+}$ is consistent with an increase in driving force with $E^{\circ\prime}$ < 1.16 V for the $Ru^{V}(O)^{3+}/Ru^{III}{-}OH^{2+}$ couple and $E^{\circ\prime}$ = 0.72 V for the $Ru^{IV}{=}O^{2+}/Ru^{II}{-}OH^{+}$ couple at pH 11.6.

$$Ru^{IV}{=}O^{2+} + HO{-}H{\cdots}OPO_3^{3-} \rightarrow Ru^{II}{-}OOH^{+} + H{-}OPO_3^{2-} \quad (5a)$$

$$Ru^{V}(O)^{3+} + HO{-}H{\cdots}OPO_3^{3-} \rightarrow Ru^{III}{-}OOH^{2+} + H{-}OPO_3^{2-} \quad (5b)$$

The dependence of k_{obs} on $[OH^-]$ was also investigated for both oxidants from pH 11.6 to 12.5 by varying the $[HPO_4^{2-}]/[PO_4^{3-}]$ ratio at $[PO_4^{3-}]$ = 5.9 mM with I = 0.25 (HPO_4^{2-}/PO_4^{3-} + KNO_3). A plot of k_{obs} vs $[OH^-]$ is shown in Figure 3. The first order dependence on $[OH^-]$, with $k_{obs} = (k_0 + k_{PO4}[5.9\ mM\ PO_4^{3-}]) + k_{OH}[OH^-]$, is consistent with OH^- acting as the buffer base or with direct attack of OH^- on $Ru^{V}(O)^{3+}$ or $Ru^{IV}{=}O^{2+}$ to give the hydroperoxide intermediates, $Ru^{III}{-}OOH^{2+}$ or $Ru^{II}{-}OOH^{+}$, eq 6, as reported

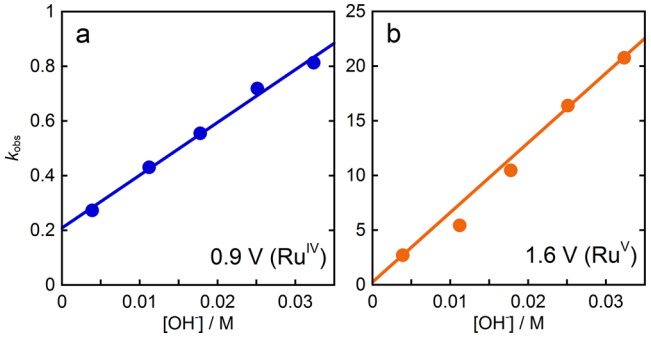

Figure 3. Plots of k_{obs} vs $[OH^-]$ for $Ru^{IV}{=}O^{2+}$ (a) and $Ru^{V}(O)^{3+}$ (b).

earlier.[8] From the slopes of the plots of k_{obs} vs $[OH^-]$ in Figure 3, $k_{Ru(IV),OH}$ = 19 M^{-1} s^{-1} and $k_{Ru(V),OH} = 6.8 \times 10^2$ M^{-1} s^{-1}.

$$Ru^{IV}{=}O^{2+} + OH^- \rightarrow Ru^{II}{-}OOH^{+} \quad (6a)$$

$$Ru^{V}(O)^{3+} + OH^- \rightarrow Ru^{III}{-}OOH^{2+} \quad (6b)$$

Following the rate-limiting O···O bond forming step, further oxidation of the coordinated peroxide intermediates leads to release of O_2 and re-entry into the catalytic cycle, eq 7.

$$Ru^{II}{-}OOH^{+} \xrightarrow{-4e^-,-3H^+,+H_2O} Ru^{IV}{=}O^{2+} + O_2 \quad (7a)$$

$$Ru^{III}{-}OOH^{2+} \xrightarrow{-4e^-,-3H^+,+H_2O} Ru^{V}{=}O^{3+} + O_2 \quad (7b)$$

In summary, our results show that $2e^-$ oxidation to $[Ru^{IV}(tpy)(bpz)(O)]^{2+}$ is sufficient to initiate water oxidation catalysis. The rate limiting step remains O---O bond formation but with $1e^-$ oxidation to Ru(III) sufficient to initiate catalysis by disproportionation to $Ru^{IV}{=}O^{2+}$. O---O bond formation is greatly accelerated with added buffer bases, reaching a turnover frequency of k_{obs} = 5.4 s^{-1} at pH 11.6 with 1 M added PO_4^{3-}. Under these conditions, both APT and direct addition of OH^- contribute significantly. The overpotential for water oxidation under these conditions is 180 mV given $E_{1/2}$ = 0.72 V for the $Ru^{IV}{=}O^{2+}/Ru^{II}{-}OH^{+}$ couple at pH 11.6.

Table 1. Rate Constant Summary for Water Oxidation by $Ru^{IV}{=}O^{2+}$ and $Ru^{V}(O)^{3+}$; I = 0.25 M (KNO_3) at 22 ± 2 °C

B	$k_{Ru(IV),B}/M^{-1}$ s^{-1}	$k_{Ru(V),B}/M^{-1}$ s^{-1}
H_2O	$k_{H2O} \approx 0.15$ s^{-1}	$k_{H2O} \approx 0.97$ s^{-1}
PO_4^{3-}	5.4	3.0×10^2
OH^-	19	6.8×10^2

Rate constants for water oxidation by both $Ru^{V}(O)^{3+}$ and $Ru^{IV}{=}O^{2+}$ are summarized in Table 1. There are notable features in these data and lessons for catalyst design: (1) The rate enhancement for O···O bond formation for OH^- compared to H_2O is notable. For $Ru^{IV}{=}O^{2+}$ as the oxidant, the rate constant ratio for oxidation of OH^- compared to oxidation of H_2O is ~1.3×10^2. It is 7.0×10^2 for $Ru^{V}(O)^{3+}$. Rate enhancements parallel proton acceptor base strength with $pK_{a,1}$ = −1.7 for H_3O^+ and 15.7 for H_2O. (2) When controlled by added buffers, *pH plays a secondary role in reactivity. Enhanced rates are due to APT and the effect of added buffer bases.* (3) At high pH, where its concentration becomes significant, OH^- may play a direct role undergoing O atom transfer and O−O bond formation with the oxo-based oxidants. (4) The importance of APT with added proton acceptor bases

dx.doi.org/10.1021/ja502637s | J. Am. Chem. Soc. 2014, 136, 6854−6857

increases with the concentration of buffer base and the pK_a of the conjugate acid. Its impact on rates can be considerable with rate constants for direct OH^- attack only 2.3−3.5 times higher than APT with PO_4^{3-} (pK_a(HPO_4^{2-}) = 12.2) as the added base. (5) At high pH, the Ru^{IV}═O^{2+} form of the catalyst $[Ru^{II}(tpy)(bpz)(OH)]^+$ is competent to carry out water oxidation with water oxidation occurring with a small overpotential. (6) Exploitation of a $1e^-$ activation mechanism for water oxidation requires a bimolecular disproportionation step for Ru(III) as shown in eq 8.

$$2Ru^{II}{-}OH_2^{2+} \xrightarrow{-2e^-} 2Ru(III) \quad (8a)$$

$$2Ru(III) \rightarrow Ru^{II}{-}OH_2^{2+} + Ru^{IV}{=}O^{2+} + 2H^+ \quad (8b)$$

■ ASSOCIATED CONTENT

Supporting Information

Preparation of *nano*ITO−RVC electrode, oxygen measurements, electrochemical and kinetic studies. This material is available free of charge via the Internet at http://pubs.acs.org.

■ AUTHOR INFORMATION

Corresponding Author

tjmeyer@unc.edu

Notes

The authors declare no competing financial interest.

■ ACKNOWLEDGMENTS

This research was supported solely by the UNC EFRC: Center for Solar Fuels, an Energy Frontier Research Center (EFRC) funded by the US Department of Energy DOE, Office of Science, Office of Basic Energy Sciences (BES) under Award DE-SC0001011.

■ REFERENCES

(1) Concepcion, J. J.; Jurss, J. W.; Brennaman, M. K.; Hoertz, P. G.; Patrocinio, A. O. T.; Murakami Iha, N. Y.; Templeton, J. L.; Meyer, T. J. *Acc. Chem. Res.* **2009**, *42*, 1954.

(2) Gagliardi, C. J.; Vannucci, A. K.; Concepcion, J. J.; Chen, Z.; Meyer, T. J. *Energy Environ. Sci.* **2012**, *5*, 7704.

(3) Dau, H.; Limberg, C.; Reier, T.; Risch, M.; Roggan, S.; Strasser, P. *ChemCatChem* **2010**, *2*, 724.

(4) Liu, X.; Wang, F. *Coord. Chem. Rev.* **2012**, *256*, 1115.

(5) Concepcion, J. J.; Jurss, J. W.; Templeton, J. L.; Meyer, T. J. *J. Am. Chem. Soc.* **2008**, *130*, 16462.

(6) Concepcion, J. J.; Jurss, J. W.; Norris, M. R.; Chen, Z.; Templeton, J. L.; Meyer, T. J. *Inorg. Chem.* **2010**, *49*, 1277.

(7) Chen, Z.; Concepcion, J. J.; Hu, X.; Yang, W.; Hoertz, P. G.; Meyer, T. J. *Proc. Natl. Acad. Sci. U.S.A.* **2010**, *107*, 7225.

(8) Vannucci, A. K.; Alibabaei, L.; Losego, M. D.; Concepcion, J. J.; Kalanyan, B.; Parsons, G. N.; Meyer, T. J. *Proc. Natl. Acad. Sci. U.S.A.* **2013**, *110*, 20918.

(9) Wang, D.; Groves, J. T. *Proc. Natl. Acad. Sci. U.S.A.* **2013**, *110*, 15579.

(10) Duan, L.; Bozoglian, F.; Mandal, S.; Stewart, B.; Privalov, T.; Llobet, A.; Sun, L. *Nat. Chem.* **2012**, *4*, 418.

(11) Duan, L.; Araujo, C. M.; Ahlquist, M. S. G.; Sun, L. *Proc. Natl. Acad. Sci. U.S.A.* **2012**, *109*, 15584.

(12) Tseng, H. W.; Zong, R.; Muckerman, J. T.; Thummel, R. *Inorg. Chem.* **2008**, *47*, 11763.

(13) Polyansky, D. E.; Muckerman, J. T.; Rochford, J.; Zong, R.; Thummel, R. P.; Fujita, E. *J. Am. Chem. Soc.* **2011**, *133*, 14649.

(14) Badiei, Y. M.; Polyansky, D. E.; Muckerman, J. T.; Szalda, D. J.; Haberdar, R.; Zong, R.; Thummel, R. P.; Fujita, E. *Inorg. Chem.* **2013**, *52*, 8845.

(15) Inoue, H.; Shimada, T.; Kou, Y.; Nabetani, Y.; Masui, D.; Takagi, S.; Tachibana, H. *ChemSusChem* **2011**, *4*, 173.

(16) Inoue, H.; Funyu, S.; Shimada, Y.; Takagi, S. *Pure Appl. Chem.* **2005**, *77*, 1019.

(17) Shimada, T.; Kumagai, A.; Funyu, S.; Takagi, S.; Masui, D.; Nabetani, Y.; Tachibana, H.; Tryk, D. A.; Inoue, H. *Faraday Discuss.* **2012**, *155*, 145.

(18) Wasylenko, D. J.; Ganesamoorthy, C.; Henderson, M. A.; Koivisto, B. D.; Osthoff, H. D.; Berlinguette, C. P. *J. Am. Chem. Soc.* **2010**, *132*, 16094.

(19) Blakemore, J. D.; Schley, N. D.; Balcells, D.; Hull, J. F.; Olack, G. W.; Incarvito, C. D.; Eisenstein, O.; Brudvig, G. W.; Crabtree, R. H. *J. Am. Chem. Soc.* **2010**, *132*, 16017.

(20) Gerli, A.; Reedijk, J.; Lakin, M. T.; Spek, A. L. *Inorg. Chem.* **1995**, *34*, 1836.

(21) Meyer, T. J.; Huynh, M. H. V. *Inorg. Chem.* **2003**, *42*, 8140.

(22) Mendez, M. A.; Alibabaei, L.; Concepcion, J. J.; Meyer, T. J. *ACS Catal.* **2013**, *3*, 1850.